

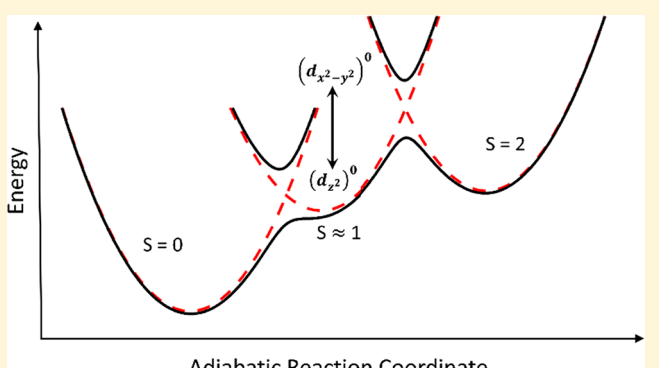
Adiabatic Ligand Binding in Heme Proteins: Ultrafast Kinetics of Methionine Rebinding in Ferrous Cytochrome c

Abdelkrim Benabbas and Paul M. Champion*

Department of Physics and Center for Interdisciplinary Research on Complex Systems, Northeastern University, Boston, Massachusetts 02115, United States

Supporting Information

ABSTRACT: The dynamics of methionine geminate recombination following photodissociation in ferrous cytochrome c is investigated over a broad temperature range. The kinetic response, above the solvent glass transition (T_{σ}) , is nearly monoexponential and displays a weak temperature dependence. Below T_{σ} , the rebinding kinetics are nonexponential and can be explained using a quenched distribution of enthalpic rebinding barriers, arising from a relatively narrow distribution of heme out-of-plane displacements. The Arrhenius prefactor of this $(\Delta S = 2)$ reaction is $\sim 10^{11}$ s⁻¹, which is similar to what has been found for the ($\Delta S = 1$) NO binding reaction in heme proteins. This observation, along with other examples of ultrafast CO binding, provides strong evidence that ligand binding to heme is an adiabatic reaction with a spin-



Adiabatic Reaction Coordinate

independent prefactor. In order to simultaneously account for the adiabatic nature of the reaction as well as the temperature dependence of both ultrafast CO and methionine geminate rebinding, it is proposed that a spin triplet state intersects and strongly couples to the reactant (S = 2) and product (S = 0) state surfaces in the transition state region along the reaction coordinate. It is also suggested that the nature of the intersecting triplet state and the reaction path may depend upon the proximity of the photolyzed ligand relative to the iron atom. At temperatures below ~60 K, the kinetic data suggest that there is either an unexpected retardation of the heme photoproduct relaxation or that heavy atom quantum mechanical tunneling becomes significant.

■ INTRODUCTION

Cytochrome c (cyt c) is an important and ubiquitous heme protein, which functions as a reversible redox carrier in electron-transport chains. It is involved in a variety of biological functions including photosynthesis, oxidative phosphorylation, and apoptosis. Both the ferric and ferrous forms of cyt c are six-coordinate, low-spin species with two endogenous ligands, histidine (His18) and methionine (Met80), bound to the heme iron. In addition, two cysteine side chains (Cys14 and Cys17) provide the thioether bridges to the heme. It was originally found that, even at pH 7, the Met80 ligand of ferrous cyt c is photolabile with a quantum yield >80% and with a geminate rebinding time of about 6 ps. 1 Recently, these results have been confirmed by other groups using different spectroscopic techniques. 2

The issues surrounding Met80 ligation in cyt c have recently been recognized as highly relevant 4-9 because this ligand can also dissociate when cyt c is bound in the mitochondrial membrane.10 The resulting five-coordinate heme then plays a key role in the apoptosis cascade. It first becomes a peroxidase⁶ and initiates peroxidation of cardiolipin in the membrane, leading to permeabilization and the release of a nitrosylated six-coordinate form of cyt c in a process related to NO synthase activity within the mitochondria.^{8,11} After release in this form, cyt c participates in formation of the apotosome, which leads to cell death. 12

Photodissociation and rebinding of diatomic ligands from heme proteins have been studied for many decades, and the pioneering contributions of the Eaton group have led to important insights concerning these fundamental biological reactions. 13-18 On the other hand, the geminate rebinding of endogenous axial ligands has been less thoroughly investigated, although the room temperature kinetics of several sixcoordinate ferrous heme proteins has been reported. 19,20 It was shown that these endogenous ligands rebind to the heme iron with a dominant and universal kinetic phase that has a time constant of $\sim 5-7$ ps at 298 K.^{1,2,19,20} It has also been hypothesized that this fast phase corresponds to the barrierless formation of a heme-ligand bond from a configuration close to the bound state.²⁰ Transient Raman investigations showed that, following Met80 photolysis in cyt c, the heme iron moves

Special Issue: William A. Eaton Festschrift

Received: July 30, 2018 Revised: September 18, 2018 Published: September 19, 2018 out of plane, leading to a domed heme configuration.² Theoretical work by Zhang et al.²¹ has used molecular dynamic simulations to study the kinetics of Met80 rebinding in cyt c. A surface hopping algorithm based on Landau—Zener theory has been applied to address the assumed nonadiabatic transition dynamics. The authors found the rebinding kinetics to be nonexponential at all temperatures with a rebinding mechanism that is distinctly different at 300 K than at lower temperatures. Additional experimental studies by Yamashita et al.²² investigated the T-dependent kinetics of methionine rebinding in WT ferrous DosH near room temperature. Their results indicate that Met rebinding is biexponential and essentially barrierless.

More recently, Solomon and co-workers⁴ analyzed the methionine binding reaction in cyt c by estimating a time-dependent local temperature for the heme that is higher than the environmental temperature. This thermal perturbation is associated with the excess energy of the absorbed photolytic photon. They suggest that endogenous ligand rebinding in cyt c can be considered as a thermal equilibrium system after \sim 2 ps and assume a time-dependent *thermal bath temperature*, allowing them to extract an equilibrium free energy for the Met80 ligand binding reaction (i.e., the so-called entatic state stabilization energy: cyt c (5C) + Met80 \leftrightarrow cyt c (6C), as described in eq 3 of the Supporting Information in ref 4).

The analysis in this study⁴ is questionable because the heme is only a small part of a nonequilibrium reacting system and its local temperature on the 1-10 ps timescale cannot be considered as the temperature of the thermal bath. The thermal bath (reservoir) in this case must include the protein and the solvent. During the first few picoseconds following the photodissociation reaction, the local heme temperature rapidly decreases, due to vibrational energy redistribution from the heme into the protein + solvent bath. The measured bound and unbound state populations on this timescale must be considered as a nonequilibrium system undergoing an essentially unidirectional rebinding reaction. The equilibrium assumption requires that multiple (i.e., bidirectional) binding and dissociation reactions are taking place on the ps timescale and that the ratio of these rates determines an equilibrium population distribution of unbound (5C) and bound (6C) heme. Because the bath (protein + solvent) is much larger than the heme, the rise in its temperature due to heme cooling is actually rather small.²³ The nonequilibrium thermal gradient between the heme and the surrounding protein + solvent bath rapidly decays to the environmental temperature, i.e., the measured temperature of the sample. Because the ratio of bound and unbound population measured during the kinetic window reflects rebinding, rather than equilibrium populations, constructing a van't Hoff plot based on the time-dependent local heme temperature does not reveal a genuine equilibrium thermodynamic free energy for the ligand binding reaction. Moreover, the values of ΔH and ΔS extracted from the van't Hoff plot for the Met80 ligand binding reaction⁴ predict a 5.7% high-spin (5C) fraction for cyt c in equilibrium at room temperature, which is not observed. 24,25

In the current study, we investigate the geminate recombination kinetics of Met80 in cyt c over a wide environmental temperature range. We show that the rebinding kinetics above the solvent glass transition $(T_{\rm g})$ is monoexponential and displays a very small enthalpic barrier compared to the thermal energy within this temperature range. On the other hand, the kinetic response below $T_{\rm g}$ is

clearly nonexponential and it can be attributed to a frozen ensemble of heme photoproduct conformations (as characterized by the heme out-of-plane equilibrium position). On the basis of the similarity between the Arrhenius prefactor found for this ($\Delta S=2$) reaction ($\sim 10^{11}~{\rm s}^{-1}$) and that of diatomic ligand binding (e.g., ${\rm NO}^{26,27}$ and ${\rm CO}^{26,28}$) to other heme proteins, with either $\Delta S=1$ or $\Delta S=2$ spin-state changes, we suggest that endogenous ligand binding in heme proteins is an adiabatic reaction with a spin-independent prefactor, as recently found for CO rebinding. Below 60 K, the measured rebinding kinetics are much faster than the prediction of the classical distributed coupling model, suggesting that either the heme photoproduct relaxation is somehow retarded or that quantum mechanical tunneling starts to compete with the classical "over-barrier reaction" at very low temperatures.

MATERIALS AND METHODS

Horse heart cytochrome c (cyt c) was purchased from Sigma-Aldrich, and it was used without further purification. Ferric cyt c was dissolved in a mixture of 25% 0.1 M phosphate buffer and 75% glycerol (vol/vol, pH 8.0). The sample was then reduced using a small amount of sodium dithionite and loaded anaerobically in a 1 mm path length home-built gold plated copper cell with two PMMA windows. The cell was then mounted on a closed cycle helium cryostat equipped with a digital temperature controller. The pump-probe setup used in this experiment is described in detail elsewhere. 19,30 Transient absorption experiments at different temperatures were performed by using two amplified and synchronized Ti:sapphire laser systems. The sample was excited with a 405 nm pump, and the change in transmission of the probe at 425 nm was detected by a photodiode connected to a lock-in amplifier. The time resolution of the system is 2.5 ps. Fast optical scanning across the sample was performed with an X-Ygalvo scanner so that fresh sample was interrogated with each pulse pair.

RESULTS

The normalized rebinding kinetics of Met80 to ferrous cyt c at temperatures above the solvent glass transition ($T_{\sigma} \cong 180 \text{ K}$) is displayed in Figure 1. Within this temperature range, the rate of Met80 geminate recombination in cyt c is weakly dependent on temperature and can be fit relatively well with a single exponential. Table S1 displays the extracted rates at each temperature. An Arrhenius plot of the rebinding rate as a function of temperature is shown in Figure 2. The enthalpic barrier (H) and the prefactor (k_0) for this reaction are found to be 0.34 \pm 0.20 kJ/mol and (1.62 \pm 0.21) \times 10¹¹ s⁻¹, respectively. The time constant for Met80 rebinding in cyt c at room temperature (296 K) was found to be 7.2 ps, which is in good agreement with previous investigations. 1-4 Figure 3 shows the kinetic traces of Met80 rebinding in cyt c below $T_{\sigma t}$ where nonexponential behavior is clearly displayed. To fit these data, we invoked a model that involves a heme conformational distribution and which has been used successfully to explain CO rebinding kinetics in a variety of heme proteins and model compounds. 19,26,28,29,31,32

The enthalpic barrier for ligand binding to heme can be formally separated into two parts²⁹

$$H = H_{\rm p} + H_{\rm D} = \frac{1}{2}Ka^2 + H_{\rm D} \tag{1}$$

The Journal of Physical Chemistry B

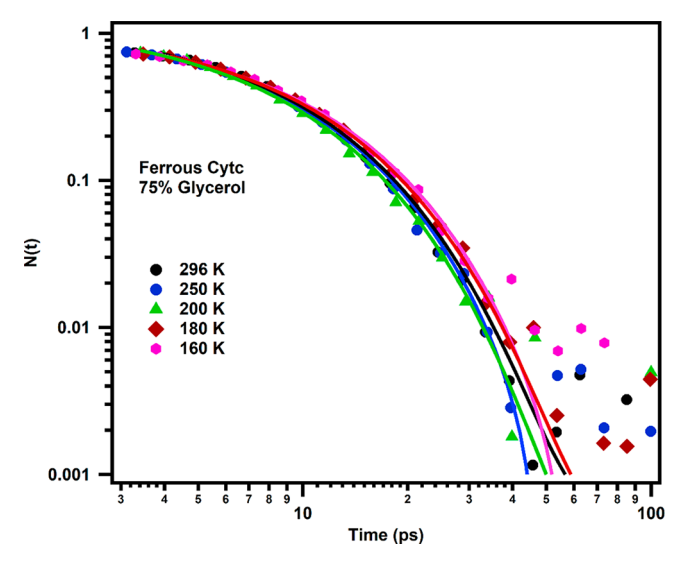


Figure 1. Geminate rebinding kinetics of the endogenous Met80 ligand in ferrous cyt c at temperatures above the glass transition temperature. The symbols represent the data, and the solid lines represent the fits to the data using a single exponential function. All kinetic data are normalized so that $N(t=0) \equiv 1$.

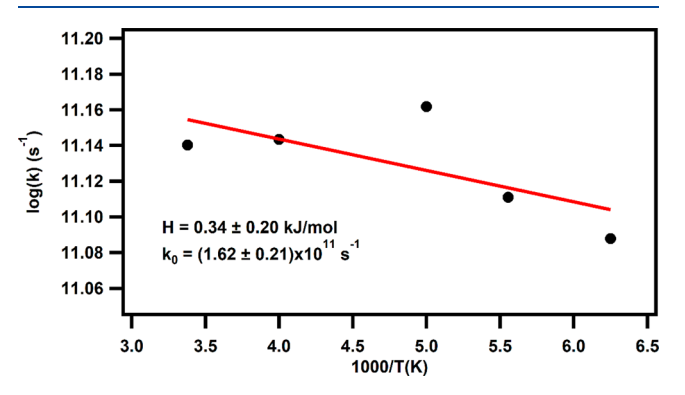


Figure 2. Arrhenius plot of Met80 rebinding in ferrous cyt c for T > 160 K. The symbols represent the measured rebinding rates, and the solid line represents the fit. The extracted Arrhenius prefactor and enthalpic barrier, along with their fitting errors, are found to be $(1.62 \pm 0.21) \times 10^{11} \, \mathrm{s}^{-1}$ and $0.34 \pm 0.20 \, \mathrm{kJ/mol}$, respectively.

where $H_{\rm P}$ primarily represents the proximal barrier due to moving the heme from the domed to the planar configuration. In this expression, a represents the overall distance that the iron needs to move relative to the heme plane during the rebinding process, while K is an "effective" force constant between the iron—protein and the iron—porphyrin that is related to the linear restoring forces in the quintet state (note that K includes a scaling factor (\lesssim 1) that accounts for the location of the reaction cusp as well as the relative energy separation between the reactant quintet state and the product singlet state along the iron—ligand coordinate 28,29).

The quantity $H_{\rm D}$ represents the remaining (a-independent) contributions to the enthalpic barrier, which primarily account for steric constraints associated with the distal pocket. For many heme systems, this term has been found to be negligible, 19,26,28,32 although, when a distal residue or substrate blocks the diatomic ligand binding site, $H_{\rm D}$ can become significant. Generally, $H_{\rm D}$ is not taken to be a Gaussian distributed parameter with significant width because the breadth and asymmetry of the rebinding barrier distribution

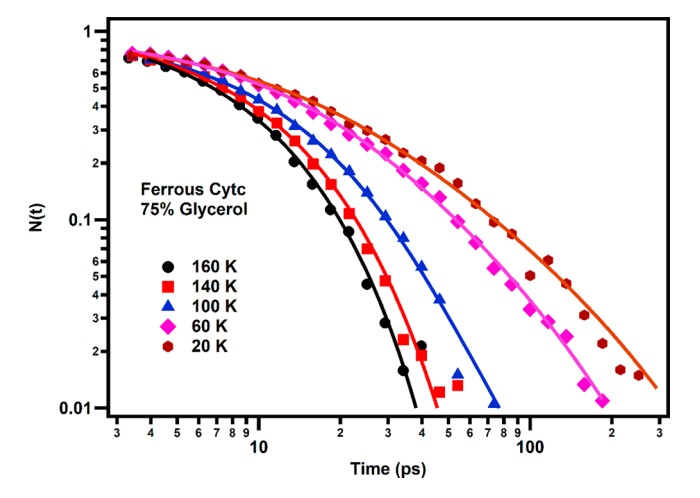


Figure 3. Geminate rebinding kinetics of Met in ferrous cyt c below the glass transition temperature, $T \le 160$ K. The symbols represent the data. The solid lines represent the fits to the data using the distributed linear coupling model, without constraint on the three fitting parameters.

due to $H_{\rm P}$ account for the nonexponential kinetics as well as being consistent with the asymmetric inhomogeneous broadening of the heme optical lineshapes^{33,34} and the associated heme iron out-of-plane displacement and its disorder.^{35–39} Thus, $H_{\rm D}$ is simply approximated by its mean value.

The distribution of the heme iron out-of-plane displacement in the photolyzed ferrous state ensemble, P(a), is taken to be a Gaussian with a mean value a_0 representing the average out-of-plane displacement and a variance σ_a describing the width of the distribution. This leads to an asymmetric distribution of barrier heights, $g(H_{\rm P})$, as given by eq S2 in the Supporting Information. The survival population of the five-coordinate photoproduct at time t after photolysis is then given by eq 2

$$N(t) = \int_0^\infty g(H_{\rm p}) \exp(-k_1 t {\rm e}^{-H_{\rm p}/k_{\rm B}T}) \, {\rm d}H_{\rm p} \eqno(2)$$

with

$$k_1 = k_0 e^{-H_D/k_B T} (3)$$

The quantity k_0 is the Arrhenius prefactor, and $k_{\rm B}$ is Boltzmann's constant. The algebraic transformations performed on eq 2 to generate a simple temperature-dependent three-parameter nonexponential fitting function are given in the Supporting Information (eq S7). The solid lines through the points in Figure 3 are the fits to the kinetic data at each different temperature. As can be seen from Figure 4, this simple distributed barrier model uses self-consistent parameters for heme doming that account very well for the low temperature nonexponential rebinding kinetics of Met80 to the heme of cyt c. The fits are distinctly superior to a stretched exponential approach, which has difficulty fitting in the long time tail of the kinetic response (as discussed in the Supporting Information of ref 19).

In Figure 4, we plot the temperature dependence of the mean iron out-of-plane displacement a_0 and its variance σ_a for Met80 binding to ferrous cyt c. The absolute values of these underlying parameters are extracted from the kinetic data for a particular choice of K, and as shown in the Supporting Information (eqs S9 and S10), they depend inversely on \sqrt{K} . Because the details of the cyt c photoproduct structure are not

The Journal of Physical Chemistry B

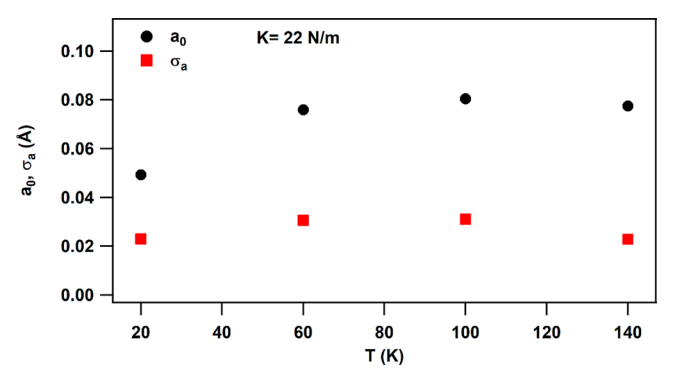


Figure 4. Temperature dependence of the average iron out-of-plane displacement a_0 and its variance σ_a as a function of temperature for Met80 rebinding in ferrous cyt c, as extracted from the kinetic data using K=22 N/m and the approach as outlined in the Supporting Information.

available, Figure 4 displays the results for K=22 N/m, which is the same value used for the heme protein CooA. ^{28,40} However, the value for K may actually need to be reduced for the endogenous Met ligand in cyt c because its transition state cusp is likely to be located at a more domed heme conformation due to a low energy triplet state intersection (vide infra). Thus, we consider K=22 N/m as an upper limit, as noted in Table 1. When the value of K is reduced to a value of K' < 22 N/m, the values of a_0 and σ_a are increased by a factor of $\sqrt{K/K'}$ in Figure 4.

In Figure 5, we display the plot of $\log_{10} k_1$ (eq 3) and the average enthalpic barrier, $\langle H \rangle$, for Met80 binding in ferrous cyt c as a function of inverse temperature. The slope of the $\log_{10} k_1$ plot yields $H_{\rm D} \sim 0$ and a prefactor $k_0 = 1.55 \times 10^{11} {\rm s}^{-1}$, which

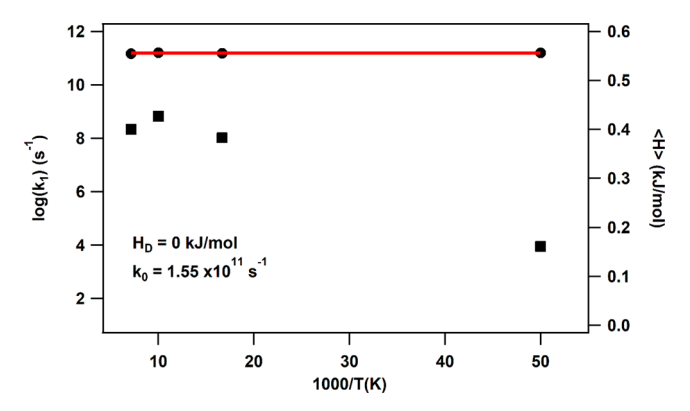


Figure 5. Temperature dependence of $\log(k_1)$ as described by eq 3 (circles) and the average enthalpic barrier, $\langle H \rangle = \frac{1}{2} K {a_0}^2 + H_{\rm D}$, for Met80 rebinding in ferrous cyt c (squares). The temperature-independent value of $\log(k_1)$ gives $H_{\rm D} \sim 0$ kJ/mol and $k_0 = 1.55 \times 10^{11} {\rm s}^{-1}$.

agrees very well with the prefactor found from the independent analysis of the high temperature kinetics based on Figure 2.

DISCUSSION

Apparent Monoexponential Behavior of the Rebinding Kinetics above T_g . Time resolved spectroscopic investigations¹⁻³ and recent ultrafast X-ray absorption studies⁴ have shown that methionine dissociation and rebinding involve a $(\Delta S = 2)$ spin transition. For the rebinding reaction, the reactant is a high-spin quintet (S = 2) and the product is a low-spin singlet (S = 0). This is analogous to heme—CO rebinding except that Met80 replaces CO, which can affect progress along the reaction coordinate because both the proximal heme distortion and the iron—ligand distance^{26,28,29} affect the heme

Table 1. Kinetic Parameters for Ligand Binding to Heme Proteins and Protoheme^a

complex	$\langle a_0 \rangle$ (Å)	$\langle \sigma_0 \rangle$ (Å)	$\langle H_{ m p} angle$	$H_{ m D}$	$\langle H \rangle$	k_0 (GHz)	references
cyt c-Met80 (T > 180 K)					0.34	162	this work
cyt c-Met80 (T < 160 K)	0.08 ^b	0.03 ^b	0.4	0	0.4	155	this work
cyt c -Met80 ($T < 160K$)	0.3 ^c	0.11 ^c	0.4	0	0.4	155	this work
$ChCooACO\ (T = 300\ K)$	0.34	0.085	7.5	0	7.5	120	28
ChCooACO (80 K < T < 180 K)	0.22	0.075	3.2	0	3.2	120	28
MbCO $(T = 295 \text{ K})$					18	1.6	59
MbCO (T < 180 K)	0.35	0.11	5.0	7	12	1.6	29
$H_2O-PPIXCO (T = 295 K)$	0.26	0.09	5.9	0	5.9	150	26
$H_2O-PPIXCO (T < 180 K)$	0.10	0.07	1.0	0	1.0	150	26
$2\text{MeIm}-\text{PPIXCO} (T < 180 \text{ K})^d$	0.30	0.14	4.0	0	4.0	150	26
$MbNO^{e}$ (T = 300 to 20 K)			0	0	0	~100	26
$H_2O-PPIXNO (T = 300 \text{ to } 20K)$			0	0	0	130	26, 27
MbO2 ^e (room temp)						~200	55

"All values of enthalpic barriers (H) are given in kJ/mol, and $T_{\rm g} \sim 180$ K is the temperature of the glass transition. $\langle H \rangle = \langle H_{\rm p} \rangle + H_{\rm D}$ and $\langle H_{\rm p} \rangle = \frac{1}{2} K a_0^2$. The values for MbCO are taken from refs 59 and 29, and the values for FePPIXCO are taken from ref 26. The values taken for K are K=14 N/m for Mb and 2MeIm-PPIX, K=27.8 N/m for H_2 O-FePPIX, and K=22 N/m for CooA. These values are consistent with a heme doming mode frequency that is usually found near 40–50 cm⁻¹. Values of a_0 and σ_a are given for cyt c-Met80 when we choose an upper limit of K=22 N/m. However, if the transition state cusp is located at a more domed heme conformation, as suggested by Figure 6, the value of K will be reduced and the relative values of a_0 and σ_a will increase as $1/\sqrt{K}$. In the alternative limit, where a fully domed heme is assumed for the cyt c-Met80 photoproduct, we take $a_0=0.3$ Å to find $\sigma_0=0.11$ Å and K=1.6 N/m. The more domed heme photoproduct conformation with a reduced value for K indicates a transition state cusp along $r_{\rm Fe-L}$ that is reflective of a constrained Fe-L distance. After relaxation at T>180 K, the 2MeIm-PPIXCO kinetics remains nonexponential but is slower than the laser repetition rate and difficult to fully analyze so that $\langle H_p \rangle \cong 8-16$ kJ/mol depending on the assumed entropic barrier. Slower than the laser repetition rate and difficult to fully analyze so that $\langle H_p \rangle \cong 8-16$ kJ/mol depending on the assumed entropic barrier. Slower than the laser repetition rate and difficult to fully analyze so that $\langle H_p \rangle \cong 8-16$ kJ/mol depending on the assumed entropic barrier. Slower than the laser repetition rate and difficult to fully analyze so that $\langle H_p \rangle \cong 8-16$ kJ/mol depending on the assumed entropic barrier. Slower than the laser repetition rate and difficult to fully analyze so that $\langle H_p \rangle \cong 8-16$ kJ/mol depending on the assumed entropic barrier. The rate of O₂ geminate rebinding to Mb at room temperature is 2×1

enthalpic barrier, H_p . The barrier for the reaction is related to the ligand field strength that is needed to vacate the high energy (e_{σ}) d-orbitals as the heme iron is driven from a domed high-spin $(d_{xy})^2(d_{xz,yz})^2(d_{z^2})^1(d_{x^2-y^2})^1$ quintet configuration to a more planar ligand-bound low-spin $(d_{xy})^2 (d_{xz,yz})^4 (d_z^2)^0 (d_x^2 - y^2)^0$ singlet configuration where the t_{2g} d-orbital subset is filled. There are at least two possible triplet configurations: $(t_{2g})^5(d_z^2)^1(d_{x^2-y^2})^0$ and $(t_{2g})^5(d_z^2)^0(d_{x^2-y^2})^1$, denoted as $(d_{x^2-y^2})^0$ and $(d_z^2)^0$ for simplicity, which may intervene during the ligand binding reaction. The mixing of these triplet states with the reactant and product spin states is governed by firstorder spin-orbit coupling, and this helps to explain the adiabatic reaction surface and spin-independent selection rules, as observed experimentally. We note that, for the heme iron atom and other biologically relevant transition metals, there can be strong dependence of the spin state with respect to small modifications in the surrounding structure and that this is consistent with entangled spin states. 41-43 In our analysis of experimental results, we consider only the most basic crystal field concepts. However, it is clear that correlation effects beyond standard density functional theory, which are associated with the subtle interplay of Coulomb repulsion and Hund's coupling, must be included in order to generate a more complete theoretical picture.⁴³

Previous investigations have shown that CO rebinding to heme proteins and heme model compounds, at both room and low temperature, is taking place via a transition state that can be described by an enthalpic barrier that is distributed due to a heterogeneous ensemble of heme out-of-plane conformations, interconverting slowly relative to the CO rebinding time-scale. 19,26,28,29,31,32 In contrast, the rebinding kinetics of Met80 in cyt c at high temperatures (Figure 1) can be fit relatively well with a single exponential and the extracted enthalpic barrier for the reaction between 160 and 298 K is very small $(H = 0.34 \pm 0.20 \text{ kJ/mol})$. To explain these results, we suggest that, because both the c-type heme and the Met80 are connected to the highly structured protein conformation, the Met80 dissociation leaves it in tight proximity to the heme iron during the 1-10 ps timescale. This can act to drive up the d_{z^2} orbital energy, forming a "reactant-like" transition state, 27,2 where the $(d_{z^2})^0$ triplet descends in energy and mixes with the singlet and quintet states, resulting in a substantial reduction of the enthalpic energy barrier. The tight proximity between the methionine sulfur and iron atoms can be inferred from the simulations of recent ultrafast X-ray absorption spectroscopy results.4 These simulations set a lower bound on the Fe-S (Met) distance in the high-spin photoproduct state to be only 2.9 Å, which is significantly shorter than the van der Waals contact distance (~3.8 Å) expected between these two atoms.

The apparent monoexponential and nearly temperatureindependent behavior of Met80 rebinding kinetics at high temperature is evidently due to the very small thermally averaged enthalpic barrier ($H = 0.34 \pm 0.20 \text{ kJ/mol}$), which is much less than the thermal energy ($k_BT \sim 1.6-2.5 \text{ kJ/mol}$) in this temperature regime. Thus, the rebinding reaction at these temperatures appears as a nearly barrierless and temperatureindependent process. This observation differs significantly from the high temperature $(T > T_g)$ CO rebinding kinetics found for CooA^{19,28} and bare heme (PPIX),²⁶ both of which display ultrafast nonexponential behavior, but with a much larger average enthalpic barrier, $\langle H \rangle \gtrsim 6$ kJ/mol.

It should be noted that the small (or nearly absent) enthalpic barrier found for the endogenous Met80 ligand could conceivably be related to a transient elevation of the local heme temperature. However, the observed, nearly exponential, kinetic response would be unlikely if local cooling on the rebinding timescale was significantly affecting the reaction. Moreover, because the heme vibrational relaxation takes place on the ~ 2 ps timescale, 45 the magnitude of the thermal increment in the surrounding protein rapidly diminishes as the vibrational energy spreads into the larger protein volume where additional structural and/or residual thermal relaxations can take place.³ The temperature increment in the protein $(\Delta T_p \sim 10 \text{ K})$ is reduced by roughly a factor of 20 compared to the heme.²³ Because of its small size and rapid equilibration with the solvent, we neglect its effect on the measured environmental temperature. In addition, the transient absorption amplitude associated with the ligand binding electronic state change is very much larger than the spectral changes due to vibrational heating, so that the detected optical transmission signal accurately reflects the time-dependent populations of the reactant and product states. Finally, the good agreement of the enthalpic barriers found in the temperature ranges 60-160 K (Figure 3) and 180-296 K (Figure 1) acts as a consistency check for the use of the environmental temperature in the kinetic analysis (vide infra).

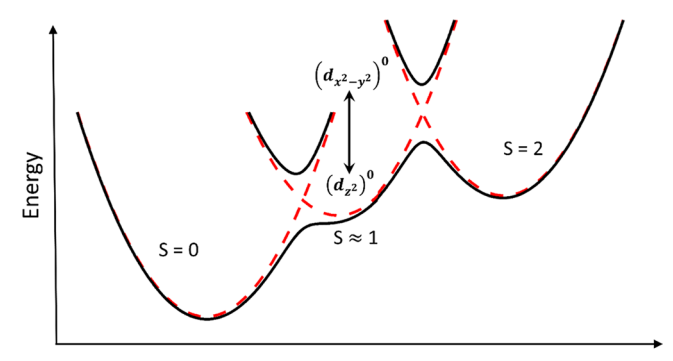
Quenched Disorder at Low Temperature. As shown in Figure 3, the kinetic response of Met80 rebinding in cyt c_1 at low temperature, is clearly nonexponential and follows the expected behavior where the rebinding kinetics slows down as the temperature decreases. This behavior mimics CO binding kinetics to heme proteins and heme model compounds, where the system undergoes the same overall spin transition ($\Delta S = 2$) during the rebinding process. This kinetic response can be quantitatively explained using the distributed linear coupling model²⁹ associated with a quenched distribution of heme geometries and proximal enthalpic barriers in the photoproduct state. As expected, the extracted average proximal heme barrier, $\langle H \rangle \sim 0.4$ kJ/mol, is nearly constant in the temperature range below T_g (down to ~40 K) and is in very good agreement with the independent value for the enthalpic barrier (0.34 \pm 0.20 kJ/mol) found at high temperature in Figure 2.

The average out-of-plane distance, a_0 , and the width of the distribution, σ_a (Figure 4), are nearly constant between 140 and 60 K and their values (based on K = 22 N/m) are ~ 0.08 and ~0.03 Å, respectively. These values are smaller by about a factor of 3 than found for CO binding to heme systems^{26,28} (see Table 1), and they are apparently reflecting that, upon methionine dissociation, the iron and sulfur atoms are held in close proximity by protein folding forces, forming a "reactantlike" transition state. 27,44 We note that the values for a_0 and σ_a can be increased if the effective force constant, K, is reduced so long as $Ka_0^2 \sim 0.8$ kJ/mol and $K\sigma_0^2 \sim 0.1$ kJ/mol, which are the unambiguous quantities determined by the kinetic data. As discussed previously,²⁹ as well as in the Supporting Information, a reduction of the "effective" force constant (K) relative to the quintet-state doming force constant (k_a) will occur as the transition state cusp is moved toward a more domed (reactant-like) heme conformation.

Adiabatic Ligand Binding in Heme Proteins. We have recently shown that CO binding to the heme iron is an adiabatic process, 28 in contrast to the commonly held view $^{46-50}$ that it is nonadiabatic due to spin-forbidden (ΔS = 2) selection rules. In this study, we find the measured Arrhenius prefactor for Met80 binding in cyt c to be $k_0 \sim 1.5 \times$ The Journal of Physical Chemistry B

10¹¹ s⁻¹. As can be seen from Table 1, the prefactor is very similar to what is found for CO and NO binding to other heme proteins (the notable exception is MbCO, where the prefactor is reduced due to an entropic barrier that has sufficient time to develop 19,26,28). The fact that NO binding involves a first-order spin-orbit coupling channel ($\Delta S = 1$) but has the same prefactor as "spin-forbidden" ($\Delta S = 2$) CO binding in a variety of systems demonstrates that the ligand binding reaction is independent of spin selection rules. All other endogenous heme ligand photolysis rebinding reactions investigated up to now involve a $\Delta S = 2$ transition, yet they rebind to the ferrous heme iron at room temperature with a dominant and universal kinetic response having a time constant of $\sim 5-7$ ps. ^{19,20} Thus, we expect that the temperature-dependent rebinding kinetics of these other heme protein systems will be similar to that of Met80 in cyt c. More specifically, the Arrhenius prefactor for these reactions is likely to be $\sim 10^{11}$ s⁻¹, which strengthens the proposition that ligand binding in ferrous heme proteins is an adiabatic process with an Arrhenius prefactor having essentially no dependence on spin selection rules. The proximity of the endogenous ligand to the iron atom can also act to increase the spin-orbit coupling matrix elements, 51,52 and when a triplet state intersection is involved, these matrix elements will be first-order (rather than second-order) in the spin-orbit coupling. This will mix the reacting states more strongly and lead to an adiabatic surface where the electrons and the associated spin-state amplitudes can instantaneously follow the nuclear motion during the reaction. It is noteworthy that frictional effects also tend to damp the magnitude of the thermal fluctuations needed for nonadiabatic surface hopping, and this also serves to move the reaction toward the adiabatic limit.53

As an example, we present a putative "reactant-like" adiabatic surface in Figure 6 where the intersections of a triplet state surface lead to the much stronger (e.g., first-order in spin-orbit coupling) spin-state mixing that is needed to create an adiabatic ground state reaction surface. In contrast, weaker coupling at the intersection point is expected for the nonadiabatic (i.e., direct $\Delta S = 2$) case, $^{46-50}$ because only second-order spin-orbit coupling is available to mix the reacting states. Figure 6 also suggests how the CO and methionine rebinding reactions can both be adiabatic but with very different reaction barriers and reaction paths. Different paths for diatomic and endogenous ligand binding are suggested by their differing kinetic responses as a function of temperature. Because the reaction coordinate path involves both heme doming and the Fe-L distance, the presence of a triplet state intersection on the adiabatic surface can lead to significant differences between the rebinding of an endogenous ligand held in close proximity to the heme iron compared to a diatomic ligand at a more distant location. In the case of methionine rebinding, the close proximity of the sulfur and iron atoms will lead to depopulation of the d_z^2 orbital and the intersection of the $(d_{z^2})^0$ triplet at relatively lower energy compared to a higher energy intersection for the $(d_{x^2-y^2})^0$ triplet. This results in a lower reaction barrier for the endogenous methionine ligand because it allows for a more domed transition state where a small in-plane heme doming fluctuation simultaneously reduces the Fe-L distance. On the other hand, the $(d_{x^2-y^2})^0$ triplet is more relevant for the adiabatic CO rebinding reaction, where the photolyzed ligand is not held in a fixed position and it can move to a more distant docking site. ⁵⁴ In this case, the $(d_{x^2-y^2})^0$ triplet configuration is



Adiabatic Reaction Coordinate

Figure 6. Proposed potential surface where the iron triplet state intersects along the reaction coordinate so that first-order spin-orbit coupling strongly mixes the spin states and leads to an ultrafast binding reaction that proceeds exclusively along the ground state adiabatic potential energy surface shown as the black solid line (not to scale), with spin-independent prefactors. The reactant (S = 2) and product (S = 0) states can still be relatively pure spin states in this adiabatic model, but in the transition region, the "triplet" state ($S \approx 1$) will very likely be a strong admixture of all three possible spin states. The restoring forces along the heme doming coordinate are expected to be larger in the bound state, but this is not shown to scale in order to more easily visualize the transition state region. The specific nature of the triplet state may depend upon the proximity of the photodissociated ligand. For endogenous ligands like methionine in cyt c, protein folding forces hold the coordinating sulfur atom very close to the iron atom⁴ and this serves to depopulate the higher lying d_{z^2} orbital so that the $(d_{z^2})^0$ triplet state is lower in energy than the $(d_{x^2-y^2})^0$ triplet state. This allows a small in-plane heme doming fluctuation to more easily admix the triplet $(d_{z^2})^0$ spin state into the ground state adiabatic reaction surface. Such a scheme can help explain the larger rebinding barrier found for CO compared to the smaller barrier found for the endogenous methionine ligand.

admixed during the in-plane heme motion along the doming coordinate, and this leads to a more planar heme in the transition state and a higher energy proximal barrier. Here it is important to note that the ultrafast optical studies do not reveal the transient population of an independent triplet state. ^{1,3,20,55} However, as shown in Figure 6, the observed two-state reaction behavior is easy to visualize for a strongly spin admixed adiabatic surface, because the triplet state intersections only take place in the transition state region.

Tunneling at Low Temperature. As can be seen from Figure 4, the parameters a_0 and σ_a , which describe the distribution of heme configurations in photolyzed cyt c below $T_{\rm g}$, are nearly constant in the temperature range 60–140 K. This is consistent with the fact that, below T_g , large conformational changes of the heme and the protein are inhibited and the distribution should be quenched. However, at 20 K, the extracted value of a_0 , found by fitting the data, becomes significantly smaller than what is found in the 60-140 K temperature range. This is a manifestation of an increase in the rebinding rate at 20 K, as can be seen from the calculated average enthalpic barrier for Met80 rebinding, which is significantly reduced at this temperature (Figure 5). This reduction in the enthalpic barrier is not expected for a classical overbarrier process where the barrier distribution should be quenched (i.e., frozen in) at all temperatures below $T_{\rm g}$.

Under the assumption that the development of the photolyzed heme conformational distribution is not retarded at these lower temperatures, the apparent reduction of the enthalpic barrier below 60 K may indicate that a heavy atom

tunneling channel becomes active in this temperature regime. A similar anomalous kinetic response at low temperature was recently observed in the case of CO binding to the transcription activator heme protein ChCooA.²⁸ The anomalous increase in the rebinding rate was attributed to the existence of a heavy atom quantum tunneling channel, which can become competitive with the classical overbarrier process at very low temperatures. In the absence of a distal barrier $(H_{\rm D})$ contribution, the crossover temperature for ChCooA, where the tunneling and the classical overbarrier rates are equal, was estimated²⁸ to be ~45 K. The crossover temperature turns out to be independent of the nature of the photodissociated ligand and the details of the proximal barrier.²⁸ It depends only on the frequency of the heme photoproduct doming mode. 28,56

The alternative possibility would involve retardation of heme relaxation and the associated development of the full photoproduct distribution below 60 K. However, because the 405 nm photon pump energy is the same at all temperatures and it contains enough excess energy to significantly heat the heme and the surrounding protein, 3,23,45,57,58 it would be surprising if the low temperature distribution was not fully established by the photoexcitation and the subsequent vibrational heating (due to nonradiative decay processes). As noted above, similar effects (i.e., faster than expected lowtemperature ligand rebinding) have been observed in CooA-CO, ²⁸ where the rebinding timescale is greater than \sim 10 ps. Because the transient thermal increment, due to the ~2 ps transfer of heme vibrational energy into the protein material, should be relatively small and fully dissipated into the solvent for $t \gtrsim 10$ ps, we assume that, although the photon-induced thermal perturbation can be important during the ultrafast heme relaxation phase, it can be considered negligible during the ligand rebinding phase.

SUMMARY

In conclusion, we have investigated the kinetics of Met80 geminate rebinding in cyt c over a wide temperature range. We found that the geminate recombination, above the solvent glass transition, is nearly monoexponential with a very small enthalpic barrier. The kinetic response below the glass transition, on the other hand, displays nonexponential and temperature-dependent behavior that is consistent with a quenched distribution of heme doming geometries in the photoproduct state. This distribution is fully consistent with the independent analysis of the high temperature kinetics. On the basis of its ultrafast timescale, we suggest that the Met80 rebinding process is best described by an adiabatic reaction surface and a "reactant-like" transition state. 44 The Arrhenius prefactor for geminate ligand binding in most ferrous heme proteins and heme model compounds, 28 including Met80 binding to cyt c, is $\sim 10^{11}$ s⁻¹. This pre-exponential rate is independent of the nature of the geminate ligand, and it does not depend on spin selection rules. Taken together, these observations indicate, quite generally, that ligand binding in heme proteins is an adiabatic process.²⁸ It is proposed that first-order spin—orbit coupling strongly mixes the reactant (S =2) and product (S = 0) spin states with a triplet state (S = 1)configuration in the transition state region and that this creates the observed adiabatic reaction surface. In addition, the specific nature of the triplet state configuration may differ and affect the rebinding barrier height, depending on the proximity of the photolyzed ligand to the iron atom. At temperatures below

~60 K, it is possible that quantum mechanical tunneling along the doming coordinate might contribute significantly to the rebinding process.

ASSOCIATED CONTENT

S Supporting Information

The Supporting Information is available free of charge on the ACS Publications website at DOI: 10.1021/acs.jpcb.8b07355.

Table displaying the rate constants of Met80 rebinding in cyt c at high temperatures and details of Met80 binding kinetic analysis using the distributed coupling model (PDF)

AUTHOR INFORMATION

Corresponding Author

*Address: Department of Physics, 111 Dana Research Center, Northeastern University, Boston, MA 02115-5000. Phone: 617.373.2918. E-mail: champ@neu.edu.

ORCID ®

Paul M. Champion: 0000-0001-6958-2836

The authors declare no competing financial interest.

ACKNOWLEDGMENTS

This work is supported by the NSF CHE-1764221.

REFERENCES

- (1) Wang, W.; Ye, X.; Demidov, A. A.; Rosca, F.; Sjodin, T.; Cao, W. X.; Sheeran, M.; Champion, P. M. Femtosecond Multicolor Pump-Probe Spectroscopy of Ferrous Cytochrome c. J. Phys. Chem. B 2000, 104, 10789-10801.
- (2) Cianetti, S.; Negrerie, M.; Vos, M. H.; Martin, J. L.; Kruglik, S. G. Photodissociation of Heme Distal Methionine in Ferrous Cytochrome c Revealed by Subpicosecond Time-Resolved Resonance Raman Spectroscopy. J. Am. Chem. Soc. 2004, 126, 13932-13933.
- (3) Negrerie, M.; Cianetti, S.; Vos, M. H.; Martin, J. L.; Kruglik, S. G. Ultrafast Heme Dynamics in Ferrous Versus Ferric Cytochrome c Studied by Time-Resolved Resonance Raman and Transient Absorption Spectroscopy. J. Phys. Chem. B 2006, 110, 12766-12781.
- (4) Mara, M. W.; Hadt, R. G.; Reinhard, M. E.; Kroll, T.; Lim, H.; Hartsock, R. W.; Alonso-Mori, R.; Chollet, M.; Glownia, J. M.; Nelson, S.; et al. Metalloprotein Entatic Control of Ligand-Metal Bonds Quantified by Ultrafast X-Ray Spectroscopy. Science 2017, 356, 1276-1280.
- (5) Abriata, L. A.; Cassina, A.; Tórtora, V.; Marín, M.; Souza, J. M.; Castro, L.; Vila, A. J.; Radi, R. Nitration of Solvent-Exposed Tyrosine 74 on Cytochrome c Triggers Heme Iron-Methionine 80 Bond Disruption: Nuclear Magnetic Resonance and Optical Spectroscopy Studies. J. Biol. Chem. 2009, 284, 17-26.
- (6) Bren, K. L.; Raven, E. L. Locked and Loaded for Apoptosis. Science 2017, 356, 1236-1236.
- (7) Godoy, L. C.; Muñoz-Pinedo, C.; Castro, L.; Cardaci, S.; Schonhoff, C. M.; King, M.; Tórtora, V.; Marín, M.; Miao, Q.; Jiang, J. F.; et al. Disruption of the M80-Fe Ligation Stimulates the Translocation of Cytochrome c to the Cytoplasm and Nucleus in Nonapoptotic Cells. Proc. Natl. Acad. Sci. U. S. A. 2009, 106, 2653-2658.
- (8) Kruglik, S. G.; Yoo, B.-K.; Lambry, J.-C.; Martin, J.-L.; Negrerie, M. Structural Changes and Picosecond to Second Dynamics of Cytochrome c in Interaction with Nitric Oxide in Ferrous and Ferric Redox States. Phys. Chem. Chem. Phys. 2017, 19, 21317-21334.
- (9) Serpas, L.; Milorey, B.; Pandiscia, L. A.; Addison, A. W.; Schweitzer-Stenner, R. Autoxidation of Reduced Horse Heart Cytochrome c Catalyzed by Cardiolipin-Containing Membranes. J. Phys. Chem. B 2016, 120, 12219-12231.

- (10) Berezhna, S.; Wohlrab, H.; Champion, P. M. Resonance Raman Investigations of Cytochrome c Conformational Change Upon Interaction with the Membranes of Intact and Ca2+-Exposed Mitochondria. *Biochemistry* **2003**, *42*, 6149–6158.
- (11) Schonhoff, C. M.; Gaston, B.; Mannick, J. B. Nitrosylation of Cytochrome c During Apoptosis. *J. Biol. Chem.* **2003**, 278, 18265—18270.
- (12) Ow, Y.-L. P.; Green, D. R.; Hao, Z.; Mak, T. W. Cytochrome c: Functions Beyond Respiration. *Nat. Rev. Mol. Cell Biol.* **2008**, *9*, 532–542.
- (13) Ansari, A.; Jones, C. M.; Henry, E. R.; Hofrichter, J.; Eaton, W. A. Conformational Relaxation and Ligand-Binding in Myoglobin. *Biochemistry* **1994**, *33*, 5128–5145.
- (14) Ansari, A.; Jones, C. M.; Henry, E. R.; Hofrichter, J.; Eaton, W. A. The Role of Solvent Viscosity in the Dynamics of Protein Conformational-Changes. *Science* **1992**, *256*, 1796–1798.
- (15) Janes, S. M.; Dalickas, G. A.; Eaton, W. A.; Hochstrasser, R. M. Picosecond Transient Absorption Study of Photodissociated Carboxy Hemoglobin and Myoglobin. *Biophys. J.* **1988**, *54*, 545–549.
- (16) Henry, E. R.; Sommer, J. H.; Hofrichter, J.; Eaton, W. A. Geminate Recombination of Carbon-Monoxide to Myoglobin. *J. Mol. Biol.* 1983, 166, 443–451.
- (17) Hagen, S. J.; Hofrichter, J.; Szabo, A.; Eaton, W. A. Diffusion-Limited Contact Formation in Unfolded Cytochrome c: Estimating the Maximum Rate of Protein Folding. *Proc. Natl. Acad. Sci. U. S. A.* **1996**, 93, 11615–11617.
- (18) Jones, C. M.; Henry, E. R.; Hu, Y.; Chan, C. K.; Luck, S. D.; Bhuyan, A.; Roder, H.; Hofrichter, J.; Eaton, W. A. Fast Events in Protein-Folding Initiated by Nanosecond Laser Photolysis. *Proc. Natl. Acad. Sci. U. S. A.* **1993**, *90*, 11860–11864.
- (19) Benabbas, A.; Karunakaran, V.; Youn, H.; Poulos, T. L.; Champion, P. M. Effect of DNA Binding on Geminate CO Recombination Kinetics in Co-Sensing Transcription Factor CooA. *J. Biol. Chem.* **2012**, 287, 21729–21740.
- (20) Vos, M. H.; Battistoni, A.; Lechauve, C.; Marden, M. C.; Kiger, L.; Desbois, A.; Pilet, E.; de Rosny, E.; Liebl, U. Ultrafast Heme-Residue Bond Formation in Six-Coordinate Heme Proteins: Implications for Functional Ligand Exchange. *Biochemistry* **2008**, *47*, 5718–5723.
- (21) Zhang, P.; Ahn, S. W.; Straub, J. E. "Strange Kinetics" in the Temperature Dependence of Methionine Ligand Rebinding Dynamics in Cytochrome C. J. Phys. Chem. B 2013, 117, 7190–7202.
- (22) Yamashita, T.; Bouzhir-Sima, L.; Lambry, J. C.; Liebl, U.; Vos, M. H. Ligand Dynamics and Early Signaling Events in the Heme Domain of the Sensor Protein Dos from Escherichia Coli. *J. Biol. Chem.* **2008**, 283, 2344–2352.
- (23) Li, P.; Champion, P. M. Investigations of the Thermal Response of Laser-Excited Biomolecules. *Biophys. J.* **1994**, *66*, 430–436.
- (24) Droghetti, E.; Oellerich, S.; Hildebrandt, P.; Smulevich, G. Heme Coordination States of Unfolded Ferrous Cytochrome c. *Biophys. J.* **2006**, *91*, 3022–3031.
- (25) Varhac, R.; Antalik, M.; Bano, M. Effect of Temperature and Guanidine Hydrochloride on Ferrocytochrome C at Neutral pH. *J. Biol. Inorg. Chem.* **2004**, *9*, 12–22.
- (26) Ye, X.; Ionascu, D.; Gruia, F.; Yu, A.; Benabbas, A.; Champion, P. M. Temperature-Dependent Heme Kinetics with Nonexponential Binding and Barrier Relaxation in the Absence of Protein Conformational Substates. *Proc. Natl. Acad. Sci. U. S. A.* **2007**, *104*, 14682–14687.
- (27) Ionascu, D.; Gruia, F.; Ye, X.; Yu, A. C.; Rosca, F.; Beck, C.; Demidov, A.; Olson, J. S.; Champion, P. M. Temperature-Dependent Studies of No Recombination to Heme and Heme Proteins. *J. Am. Chem. Soc.* **2005**, *127*, 16921–16934.
- (28) Benabbas, A.; Sun, Y. H.; Poulos, T. L.; Champion, P. M. Ultrafast CO Kinetics in Heme Proteins: Adiabatic Ligand Binding and Heavy Atom Tunneling. *J. Am. Chem. Soc.* **2017**, *139*, 15738–15747.

- (29) Srajer, V.; Reinisch, L.; Champion, P. M. Protein Fluctuations, Distributed Coupling, and the Binding of Ligands to Heme Proteins. *J. Am. Chem. Soc.* **1988**, *110*, 6656–6670.
- (30) Yu, A.; Ye, X.; Ionascu, D.; Cao, W.; Champion, P. M. Two-Color Pump-Probe Laser Spectroscopy Instrument with Picosecond Time-Resolved Electronic Delay and Extended Scan Range. *Rev. Sci. Instrum.* 2005, 76, 114301–114308.
- (31) Karunakaran, V.; Benabbas, A.; Sun, Y. H.; Zhang, Z. Y.; Singh, S.; Banerjee, R.; Champion, P. M. Investigations of Low-Frequency Vibrational Dynamics and Ligand Binding Kinetics of Cystathionine Beta-Synthase. *J. Phys. Chem. B* **2010**, *114*, 3294–3306.
- (32) Benabbas, A.; Ye, X.; Kubo, M.; Zhang, Z. Y.; Maes, E. M.; Montfort, W. R.; Champion, P. M. Ultrafast Dynamics of Diatomic Ligand Binding to Nitrophorin 4. *J. Am. Chem. Soc.* **2010**, *132*, 2811–2820
- (33) Srajer, V.; Champion, P. M. Investigations of Optical-Line Shapes and Kinetic Hole Burning in Myoglobin. *Biochemistry* **1991**, 30, 7390–7402.
- (34) Srajer, V.; Schomacker, K. T.; Champion, P. M. Spectral Broadening in Biomolecules. *Phys. Rev. Lett.* **1986**, *57*, 1267–1270.
- (35) Parak, F.; Knapp, E. W. A Consistent Picture of Protein Dynamics. *Proc. Natl. Acad. Sci. U. S. A.* 1984, 81, 7088–7092.
- (36) Frauenfelder, H.; Petsko, G. A.; Tsernoglou, D. Temperature-Dependent X-Ray-Diffraction as a Probe of Protein Structural Dynamics. *Nature* **1979**, 280, 558–563.
- (37) Leu, B. M.; Zhang, Y.; Bu, L. T.; Straub, J. E.; Zhao, J. Y.; Sturhahn, W.; Alp, E. E.; Sage, J. T. Resilience of the Iron Environment in Heme Proteins. *Biophys. J.* **2008**, *95*, 5874–5889.
- (38) Vojtechovsky, J.; Chu, K.; Berendzen, J.; Sweet, R. M.; Schlichting, I. Crystal Structures of Myoglobin-Ligand Complexes at near-Atomic Resolution. *Biophys. J.* **1999**, *77*, 2153–2174.
- (39) Kachalova, G. S.; Popov, A. N.; Bartunik, H. D. A Steric Mechanism for Inhibition of CO Binding to Heme Proteins. *Science* **1999**, 284, 473–476.
- (40) Karunakaran, V.; Benabbas, A.; Youn, H.; Champion, P. M. Vibrational Coherence Spectroscopy of the Heme Domain in the Co-Sensing Transcriptional Activator CooA. *J. Am. Chem. Soc.* **2011**, *133*, 18816–18827.
- (41) Kurashige, Y.; Chan, G. K.-L.; Yanai, T. Entangled Quantum Electronic Wavefunctions of the Mn4cao5 Cluster in Photosystem Ii. *Nat. Chem.* **2013**, *5*, 660.
- (42) Sharma, S.; Sivalingam, K.; Neese, F.; Chan, G. K.-L. Low-Energy Spectrum of Iron—Sulfur Clusters Directly from Many-Particle Quantum Mechanics. *Nat. Chem.* **2014**, *6*, 927.
- (43) Weber, C.; O'Regan, D. D.; Hine, N. D.; Littlewood, P. B.; Kotliar, G.; Payne, M. C. Importance of Many-Body Effects in the Kernel of Hemoglobin for Ligand Binding. *Phys. Rev. Lett.* **2013**, *110*, 106402.
- (44) Szabo, A. Kinetics of Hemoglobin and Transition-State Theory. *Proc. Natl. Acad. Sci. U. S. A.* **1978**, *75*, 2108–2111.
- (45) Mizutani, Y.; Kitagawa, T. Direct Observation of Cooling of Heme Upon Photodissociation of Carbonmonoxy Myoglobin. *Science* **1997**, 278, 443–446.
- (46) Harvey, J. N. Understanding the Kinetics of Spin-Forbidden Chemical Reactions. *Phys. Chem. Chem. Phys.* **2007**, *9*, 331–343.
- (47) Harvey, J. N. Spin-Forbidden CO Ligand Recombination in Myoglobin. *Faraday Discuss.* **2004**, 127, 165–177.
- (48) Franzen, S. Spin-Dependent Mechanism for Diatomic Ligand Binding to Heme. *Proc. Natl. Acad. Sci. U. S. A.* **2002**, *99*, 16754–16759.
- (49) Redi, M. H.; Gerstman, B. S.; Hopfield, J. J. Hemoglobin Carbon-Monoxide Binding Rate Low-Temperature Magneto-Optical Detection of Spin-Tunneling. *Biophys. J.* **1981**, *35*, 471–484.
- (50) Jortner, J.; Ulstrup, J. Dynamics of Non-Adiabatic Atom Transfer in Biological-Systems Carbon-Monoxide Binding to Hemoglobin. *J. Am. Chem. Soc.* **1979**, *101*, 3744–3754.
- (51) Cave, R. J.; Newton, M. D. Calculation of Electronic Coupling Matrix Elements for Ground and Excited State Electron Transfer

Reactions: Comparison of the Generalized Mulliken-Hush and Block Diagonalization Methods. *J. Chem. Phys.* **1997**, *106*, 9213–9226.

- (52) Kiefer, P. M.; Hynes, J. T. Kinetic Isotope Effects for Nonadiabatic Proton Transfer Reactions in a Polar Environment. 2. Comparison with an Electronically Diabatic Description. *J. Phys. Chem. A* **2004**, *108*, 11809–11818.
- (53) Frauenfelder, H.; Wolynes, P. G. Rate Theories and Puzzles of Hemeprotein Kinetics. *Science* **1985**, 229, 337–345.
- (54) Lim, M.; Jackson, T. A.; Anfinrud, P. A. Binding of CO to Myoglobin from a Heme Pocket Docking Site to Form Nearly Linear Fe-C-O. *Science* **1995**, 269, 962–966.
- (55) Ye, X.; Demidov, A.; Champion, P. M. Measurements of the Photodissociation Quantum Yields of MbNO and MbO₂ and the Vibrational Relaxation of the Six-Coordinate Heme Species. *J. Am. Chem. Soc.* **2002**, *124*, 5914–5924.
- (56) Rosca, F.; Kumar, A. T. N.; Ionascu, D.; Ye, X.; Demidov, A. A.; Sjodin, T.; Wharton, D.; Barrick, D.; Sligar, S. G.; Yonetani, T.; et al. Investigations of Anharmonic Low-Frequency Oscillations in Heme Proteins. *J. Phys. Chem. A* **2002**, *106*, 3540–3552.
- (57) Henry, E. R.; Eaton, W. A.; Hochstrasser, R. M. Molecular-Dynamics Simulations of Cooling in Laser-Excited Heme-Proteins. *Proc. Natl. Acad. Sci. U. S. A.* **1986**, 83, 8982–8986.
- (58) Schomacker, K. T.; Champion, P. M. Investigations of Spectral Broadening Mechanisms in Biomolecules Cytochrome c. *J. Chem. Phys.* **1986**, *84*, 5314–5325.
- (59) Tian, W. D.; Sage, J. T.; Srajer, V.; Champion, P. M. Relaxation Dynamics of Myoglobin in Solution. *Phys. Rev. Lett.* **1992**, *68*, 408–411.
- (60) Gruia, F.; Ye, X.; Ionascu, D.; Kubo, M.; Champion, P. M. Low Frequency Spectral Density of Ferrous Heme: Perturbations Induced by Axial Ligation and Protein Insertion. *Biophys. J.* **2007**, *93*, 4404–4413.